

Polar-discontinuity-retaining A-site intermixing and vacancies at SrTiO₃/LaAlO₃ interfacesV. Vonk,^{1,2,*} J. Huijben,³ D. Kukuruznyak,¹ A. Stierle,^{1,4} H. Hilgenkamp,³ A. Brinkman,³ and S. Harkema³¹Max Planck Institute for Metals Research, Stuttgart, Germany²Radboud University Nijmegen, Institute for Molecules and Materials, Nijmegen, The Netherlands³MESA + Institute for Nanotechnology, University of Twente, Enschede, The Netherlands⁴Universität Siegen, Siegen, Germany

(Received 23 November 2011; revised manuscript received 15 December 2011; published 3 January 2012)

Our anomalous surface x-ray diffraction study of the interface between SrTiO₃(001) substrates and thin polar films of LaAlO₃ shows La/Sr interdiffusion leading to neutrally charged Sr_{1-1.5x}La_xO layers. From a thickness of two unit cells, the LaAlO₃ film's interior retains its polar stacking sequence, which is compensated by a cationic compositional change of the substrate's terminating TiO₂ layer. While such valence-retaining A-site intermixing does not resolve the polar catastrophe, it may be a general feature at oxide interfaces influencing the electronic and magnetic properties.

DOI: [10.1103/PhysRevB.85.045401](https://doi.org/10.1103/PhysRevB.85.045401)

PACS number(s): 68.47.Gh, 61.05.cf, 68.35.Dv

I. INTRODUCTION

Interfaces between perovskite-related materials disclose unanticipated physical properties. Whereas these compounds, with the general formula ABO_3 , are of great interest for their richness in bulk properties, over the past years it has been identified that surfaces and interfaces add another dimension to their phase diagrams. One of the most intriguing examples is SrTiO₃(001) (STO) and its interface with LaAlO₃ (LAO). This interface possesses a two-dimensional electron gas (2DEG), which shows conduction,¹ superconductivity,² and even magnetic effects,^{3,4} properties that are absent in the bulk of both wide-band-gap insulating compounds. Interestingly, the 2DEG is absent in LAO films thinner than four unit cells,⁵ unless it is capped by STO.⁶

The nominal interface is characterized by a transition from a nonpolar (STO) to a polar (LAO) crystal structure, which introduces a diverging electrostatic energy. In the so-called electronic reconstruction scenario, it is proposed that valence changes of the interfacial titanium from 4+ to 3+ can annihilate the polar instability and form a 2DEG.⁷ It has also been proposed that new conducting phases could form, either by oxygen vacancies⁸⁻¹⁰ or by atomic intermixing,¹¹ the latter of which has been confirmed with a variety of techniques.¹² It remains unclear how these scenarios can be reconciled with the thickness-dependent insulator-conductor transition, since doping in these cases is expected for any film thickness. Several papers address this problem, thereby focusing on electronic reconstruction^{13,14} or oxygen vacancies.^{15,16}

Transport measurements reveal interfacial carrier concentrations much lower than what is predicted by electronic reconstruction,⁶ whereas spectroscopic studies indicate both localized and itinerant Ti 3d states.¹⁷ Others report the absence of band bending and band offsets,¹⁸ which would be expected within the electronic reconstruction scenario.

In order to understand the atomic intermixing and its relation with the doping mechanism, we make use of anomalous surface x-ray diffraction (SXRD), focusing in particular on the cationic composition at the A sites. The most important result is that La doping of the substrate leads to a vacancy-rich A-site composition of Sr_{1-1.5x}La_x, the formation of which already starts at the onset of deposition. The uncovered A-site

compositions do not take away the polar instability, which thus still requires a change from the nominal structure and/or composition at the B sites. Our data show evidence for such a mechanism starting at a thickness of three unit cells.

II. EXPERIMENT AND RESULTS**A. Sample preparation**

Thin films of LAO with thicknesses of one to five unit cell layers (hereafter referred to as 1–5UC) were grown on single TiO₂-terminated STO(001) substrates (Crystec) by pulsed laser deposition (PLD) at an oxygen pressure of 3×10^{-5} mbar. This intermediate pressure is high enough to avoid bulk substrate conductivity by oxygen vacancies and allows for comparison with other studies.

Single TiO₂-terminated STO substrates were obtained by a well-established wet chemical etching procedure.¹⁹ During the deposition of the thin films, use of reflection high-energy electron diffraction (RHEED) enabled unit cell thickness control by counting intensity oscillations. The oxygen partial pressure during deposition was kept at 3×10^{-5} mbar, while the substrate temperature was 1043 K. During cool-down to room temperature, the oxygen pressure was increased to 400 mbar and each sample was kept at 873 K for 1 h in order to maximize oxidation. After growth, the surfaces of the films are characterized by atomic force microscopy (AFM), which shows a terrace-step structure. Typical step heights are 4 Å, which is an indication that the substrate's step height is maintained after overgrowth by LAO.

B. Data collection and fitting including anomalous CTR's

Crystal truncation rod (CTR) data sets on the various samples were obtained at the MPI-MF beamline at the Ångström Quelle Karlsruhe (ANKA), Germany.²⁰ The CTR data were integrated and corrected,²¹ resulting in sets of structure factors. For samples 1UC and 5UC, further data were collected at an x-ray energy of 6.28 keV probing the La-L₁ absorption edge. Structure refinement for these samples was carried out using the anomalous and nonanomalous data simultaneously, which prevents large correlations between the occupancies of Sr and La at the A sites.²² This unwanted

TABLE I. Results of the data collections and structure refinements of the various samples. Listed are the total number of data points and unique points after merging using space group $P4mm$. CTR's were measured at 10.00 keV. For samples 1UC and 5UC, the second values give the number of data points collected at the La- L_1 absorption edge. The value R_{merge} indicates the agreement between different symmetry-equivalent points. Structural models with p parameters are fitted to all the data, resulting in a single χ^2 value.

Sample	Data points	Unique points	R_{merge}	p	χ^2 ^a
1UC	192 + 532	80 + 107	0.172 + 0.165	19	0.92
1UC (90 K)	80	80		19	1.8
2UC	642	149	0.157	23	0.60
3UC	835	196	0.192	20	0.91
4UC	707	201	0.099	27	2.0
5UC	1225 + 532	228 + 107	0.08 + 0.234	37	2.7

^a $\chi^2 = \frac{1}{N-p} \sum_{hkl} \frac{(|F_{\text{obs}} - s_E F_{\text{calc}}|)^2}{\sigma(F_{\text{obs}})^2}$, with N the number of measurements, p the number of parameters, F the structure factor, and s_E the scale factor for the particular x-ray energy.

effect is due to the similarity in the atomic scattering factors (f_a) of Sr and La [$|f_{\text{La}} - 1.5f_{\text{Sr}}| \leq 2$ for $0 < \sin(\theta)/\lambda < 1$]. For example, the scattering by a site occupancy of $\text{La}_x\text{Sr}_{1-1.5x}$ is indistinguishable from an A site fully occupied by Sr. Only by including data taken at the absorption edge of one of the two elements, thereby altering f_a , can a unique solution for the site occupancies be found. In order to rule out the effect of enlarged thermal diffuse scattering, for sample 1UC data were taken at 90 K as well. Refinement of the low-temperature data did not reveal any anomaly compared to room temperature, and essentially the same composition and atomic positions were found.

Results of data reduction and fitting using space group $P4mm$ are listed in Table I. Exemplary CTR's for samples 1–5UC are shown in Fig. 1. A modified version of the program ROD (Ref. 23) is used to fit structural models to the CTR data.²⁴ The supplemental material²⁵ lists the refined structural parameters for all samples.

C. X-ray reflectivity

X-ray reflectivity (XRR) curves (see Fig. 2) taken at 10.0 and 6.28 keV of sample 5UC show a striking difference

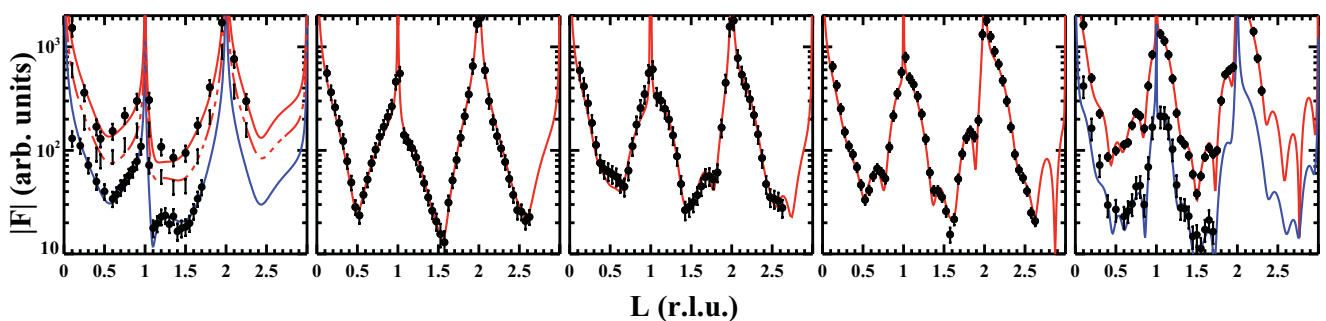


FIG. 1. (Color online) Crystal truncation rod data (dots) and fits (lines). Shown are the (2,0) rods for samples 1UC (left) to 5UC (right). Fits to the nonanomalous data are red (upper) and those to the anomalous data are blue (lower). For sample 1UC, the 90 K data are shown by a dotted dashes.

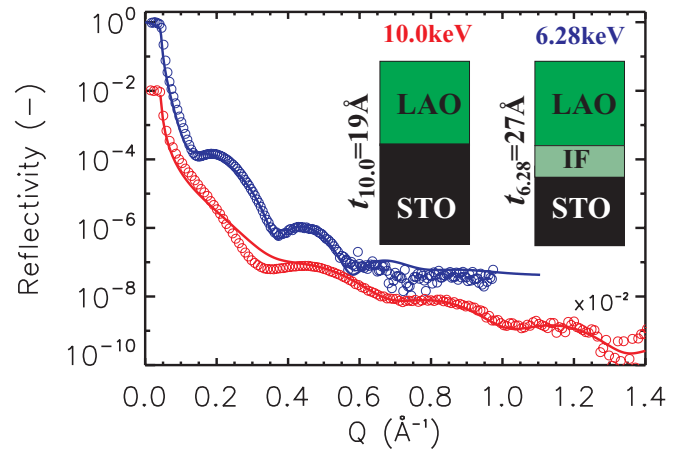


FIG. 2. (Color online) X-ray reflectivity curves of the nominally five-unit-cell thin film, taken at two different x-ray energies. Open circles show the data points taken at $E = 6.28$ keV (blue, upper) and $E = 10.0$ keV (red, lower) and their corresponding fits (solid lines). The inset shows schematically the structure of the film whereby the colors indicate the effective scattering density ρ' that is probed at each x-ray energy. The interface (IF) has a significantly different ρ' at the La- L_1 edge.

that is indicative of La interdiffusion. The apparent thickness as “seen” by the x-ray beam is different for the two x-ray energies, although they are taken from the same sample. Since the difference between the two curves is determined only by the anomalous scattering of La, it must follow that the difference between the two fitted thicknesses ($t_{6.28} = 27$ Å and $t_{10.0} = 19$ Å) of 8(2) Å is the La interdiffusion depth.

In the XRR regime, the derivative $d\rho'/dz$ of the scattering density ρ' is probed. Far away from resonances, the scattering density is equal to the electron density ρ . Close to resonances, the scattering density can be obtained by correcting ρ with f' and f'' , which account for the dispersion and absorption. Our results indicate that at 10.0 keV, there is hardly any difference in density between the STO substrate and the interdiffusion region, whereas at the La L_1 edge the contrast between the substrate and the interdiffusion region is substantial. The fit to the 10.0 keV data shows some deviation around $Q = 0.2$. This is an indication that the real interdiffusion profile is not very accurately described by the used error function. Nevertheless,

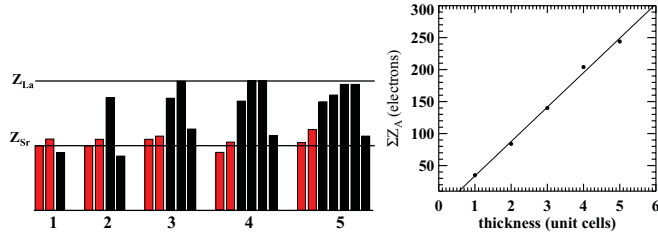


FIG. 3. (Color online) (Left) Electron weight at the various A sites ($Z_A = \theta_{\text{Sr}}Z_{\text{Sr}} + \theta_{\text{La}}Z_{\text{La}}$). Shown are the results for all the thicknesses of one to five unit cells; A sites in the substrate are in red (bright), those in the film are black (dark). The levels of $Z_{\text{Sr}} = 38$ and $Z_{\text{La}} = 57$ are indicated for comparison. Errors are 5%–10% of the values. (Right) Sum of the total electron weight at the A sites ($\sum Z_A$) as a function of the film thickness. The solid line is a linear fit as described in the text.

the period of the thickness oscillations is well reproduced, and it is not expected that more complicated interdiffusion profiles will change that.

D. Thickness-dependent composition

Figure 3 shows the A-site electron occupation Z_A in the different films obtained from fits to the CTR data whereby $Z_A = \theta_{\text{Sr}}Z_{\text{Sr}} + \theta_{\text{La}}Z_{\text{La}}$, with occupancies θ , $Z_{\text{Sr}} = 38$, and $Z_{\text{La}} = 57$. It is important to note that a value of Z_A close to 57 means that the site is (almost) completely occupied by La, and that no Sr can be present. From a thickness of three unit cells, atomic layers with A sites almost fully occupied by La occur. The results also show that the A sites in the outermost film layers are all close to $Z_A = 38$, the same value as in the substrate.

The A-site electron occupation summed over all layers within one film, $\sum Z_A$, is plotted in Fig. 3. A linear relation as a function of film thickness is found, of which the slope is $54(2) \#e/(\text{unit cell layer})$ and the offset $-20(7) \#e$. From the slope it can be concluded that, as expected, with the growth of each unit cell LAO, one complete layer of La atoms ($57\#e$) is deposited. The negative offset means that some of the heavier La disappears from the film and is partially replaced by the lighter Sr. This exchange of Sr and La starts already with growth of the first unit cell layer and seems not to change anymore with increasing film thickness. The A-site compositions summed over all film layers in samples 1UC and 5UC are $\text{La}_{0.2}\text{Sr}_{0.7}$ and $\text{La}_{4.1}\text{Sr}_{0.3}$, respectively. We estimate that the error in the total composition per element will be around $\sqrt{n}0.1$, where n is the number of unit cell layers.²⁵ This means that we find a significant La deficiency with respect to the films' nominal compositions. Furthermore, we find that a fraction of the La that disappears from the film stays within two STO unit cells from the interface region, and the rest diffuses much deeper into the substrate. This exchange of Sr and La results in a film and near-interface region containing an appreciable amount of vacancies, which can only be explained by segregation and accumulation of bulk STO A-site vacancies.

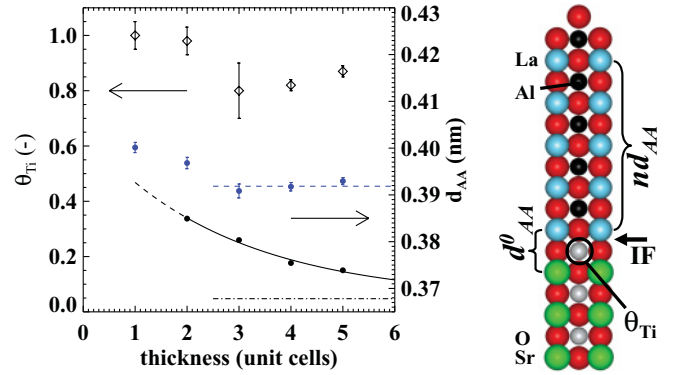


FIG. 4. (Color online) (Left) Averaged distances between A sites (d_{AA}) as a function of the film thickness (lower black dots). The values for d_{AA} follow an exponential decay (black solid line) to $3.68(7) \text{ \AA}$ for thick films (black dash-dotted line) as described in the text. Also shown are the values for the distance across the interface of the substrate and film d_{AA}^0 (middle blue dots). Values of d_{AA}^0 level off to $3.92(2) \text{ \AA}$ (dashed line). The diamonds (black, upper) give the refined occupancies θ of the interfacial Ti atoms. (Right) Schematic atomic model for an n unit cell thin LAO film and its nominal interface (IF) with STO.

E. Strain and relaxation

Figure 4 shows the average distances between the A sites, d_{AA} , along the growth direction for each film. Values for the distance across the nominal interface with STO, d_{AA}^0 , are shown separately in Fig. 4. We find an exponential relation for d_{AA} as a function of thickness with a characteristic decay of $2.7(2)$ unit cells and a thick-film limit of $3.68(7) \text{ \AA}$. The characteristic thickness coincides roughly with the reported insulator-conductor transition.⁵ The thick-film limit is very close to the expected c -axis lattice parameter of 3.71 \AA for a LAO film fully strained to STO, as explained below. The values of d_{AA}^0 are significantly larger than d_{AA} and level off at $3.92(2) \text{ \AA}$ from a thickness of three unit cells. This enlarged distance cannot be caused by strain, but is an indication that the interfacial atomic configuration differs from the substrate and film. Nominally the TiO_2 layer is flanked by a SrO and a LaO layer, whereas within the film (compositionally) equal A-site layers are expected. Such symmetry breaking has been found to result in enlarged AO-BO₂ distances in bulk $\text{La}_{0.6}\text{Sr}_{0.1}\text{TiO}_3$.²⁶

The heterointerface marks the transition between two intrinsically different crystal symmetries: $Pm\bar{3}m$ in the substrate and $R\bar{3}c$ in the film, whereby thin films are expected to adapt to the substrate. The cations in bulk LAO occupy atomic positions on a bcc-based lattice, just as in the perfect perovskite structure. The rhombohedral crystal structure is determined merely by small deviations of the oxygen positions from cubic symmetry by tilts. Around 821 K, LAO shows a phase transition to cubic.²⁷ If the LAO film were completely relaxed and adopted its own bulk symmetry, owing to the oxygen tilt system, very weak reflections would be present in addition to the main perovskite peaks. For none of the films investigated here have we found such reflections, and the data were merged using space group $P4mm$ with a single perovskite cell. Also, the low-temperature measurements at 90 K of sample 1UC showed no additional reflections. It could still be that the extra

reflections are present but too weak to be detected. There were also no signs for in-plane lattice relaxation, which would be expected above the critical thickness for the formation of misfit dislocations. Therefore, we assume the films here to be pseudomorphic, also with respect to the oxygen octahedra network.

The out-of-plane film lattice parameter is shown to exponentially approach the nonbulk value of $3.68(7)$ Å with increasing film thickness. This thick-film limit c axis corresponds to the value expected for the film's pseudomorphic state. Taking a Poisson ratio of $\nu = 0.26$ (Ref. 28) and in-plane tensile strain $\epsilon = +0.030$ for the LAO film results in an expected strained c axis of 3.71 Å.

III. DISCUSSION

It has been found in other studies that indeed La can diffuse deeply into the STO.¹² We find significant amounts of La in the first two STO substrate unit cell layers, which means that probably the La level in the deeper layers is below the sensitivity of SXRD. Cationic diffusion in La-doped STO has been discussed to be an A -site vacancy-mediated hopping mechanism, which increases with La doping levels.²⁹ It has also been suggested that for La-doped STO, there exist two charge-compensating mechanisms, electronic (Ti valence changes) and ionic (expulsion of Sr), which depend on the oxygen partial pressure.³⁰ Heating under oxidative conditions of La-doped STO leads to SrO outgrowth on the surface, and should result in a substrate composition $\text{Sr}_{1-1.5x}\text{La}_x\text{TiO}_3$.³¹ Here we indeed find this composition, but only in a thin region close to the interface. It is very likely that this thickness depends on temperature and oxygen pressure. Including surface Sr islands in the fit models yielded insignificant coverages, which means that the amount of Sr is below the detection limit, or that Sr does not order epitaxially on top of the films.

In an earlier paper, we reported on the LAO/STO interface structure during PLD of the first unit cell layer.³² Also there it was found that the occupancy of the atoms in the overlayer was close to 0.5, and this was interpreted as an incomplete unit cell layer. In fact, this is completely in line with the present results, only the less-than-unity occupancies should be interpreted as being atomic vacancies instead of island coverages.³³ The earlier *in situ* SXRD measurements corroborate the present study's outcome that A -site interdiffusion appears with deposition of the very first layer.

Diffusion of La into the substrate leads to a nonpolar structure in the form of $(\text{Sr}_{1-1.5x}\text{La}_x)^{2+}\text{O}^{2-}$ layers. The LAO film does contain a polar stacking, which requires that compensating charges of $\pm 0.5e$ exist on both its interfaces.⁷ First, we focus on the films' terminating unit cell layers, i.e., at their free surfaces. Our data indicate that these contain neutrally charged AO layers. It is most likely that also the outermost BO_2 layers and oxygen atoms together form a charge-neutral film termination. It is unlikely that a charged layer would follow the neutral AO layer and terminate the crystal. A compensating charge of $-0.5e$ should therefore be formed on the second to last BO_2 layer, which is possible in the form of oxygen vacancies. Indeed, refinement of the oxygen occupancies in this layer results in values close to the expected

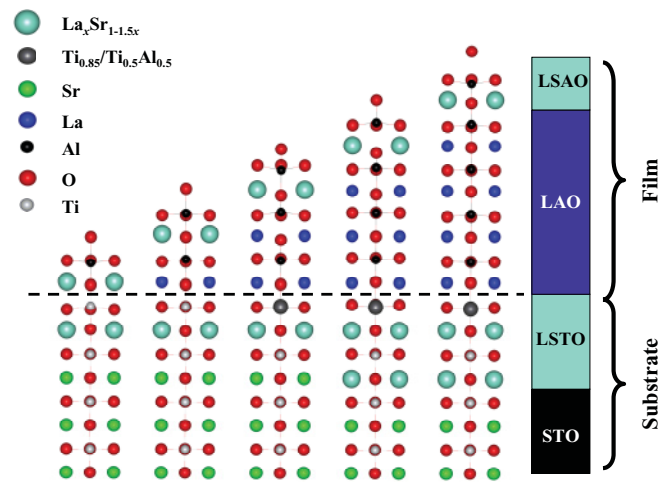


FIG. 5. (Color online) Schematic view along the (100) direction of the final atomic structures of samples 1UC (left) to 5UC (right). The dotted line indicates the nominal interface. The A sites with an occupancy $\text{Sr}_{1-1.5x}\text{La}_x$ are drawn by the largest spheres. The change at the interfacial Ti site from a film thickness of three unit cells is indicated by an enlarged darker sphere.

7/8. Next we consider the film-substrate interface where La/Sr intermixing takes place. In principle, intermixing does not take away the diverging electrostatic energy, but would merely smear out the potential buildup at that particular interface.⁷ An offset of $\pm 0.5e$ is still necessary. Since our data indicate that this offset is not dictated by the interfacial AO layers, it must appear on the nearby BO_2 layers. Oxygen vacancies in this layer would cause a positive charge, whereas a negative charge is required. For the purpose of investigating the composition of the substrate's terminating BO_2 layer, its Ti occupancy is refined. The results in Fig. 4 show that from a thickness of three unit cells, the Ti occupancy drops to about 0.85. This decreased scattering power is due either to the appearance of B -site vacancies or to intermixing with the lighter element Al. Assuming vacancies, a composition of $\text{Ti}_{0.85}\text{O}_2$ would result in a charge of $-0.6e$ for this layer. In the case of Ti/Al intermixing, the scattering power of $\text{Ti}_{0.85}\text{O}_2$ is almost indistinguishable from that of a composition $\text{Ti}_{0.5}\text{Al}_{0.5}\text{O}_2$, which would have a charge of $-0.5e$. Both scenarios would provide the required $-0.5e$ charge and compensate for the film's electrostatic energy buildup.

The picture of the thin-film atomic structure that emerges from our study is schematically shown in Fig. 5. Deposition of LAO on STO leads immediately to La/Sr intermixing, thereby forming charge-neutral $\text{La}_x\text{Sr}_{1-1.5x}\text{O}$ layers and a nonconducting phase. This charge-neutral layer is found in the substrate but also in the topmost AO layer of the films. From a thickness of two unit cells, La-rich layers are formed and with that a polar film stacking. From a thickness of three unit cells, we find a compositional change at the substrate's terminating B sites, which annihilates the diverging electrostatic energy. These results show that the expected potential buildup over the interface of 1–5UC thin films is for a large part structurally compensated. However, these results cannot rule out that electronic reconstruction, albeit in much weaker form, is the mechanism responsible for the 2DEG formation.

Vacancies play a role in LAO surface reconstructions,³⁴ STO grain boundaries,³⁵ and they could be responsible for inhomogeneities by clustering.³⁶ They also contribute to the strain state,³⁷ and could therefore play a role in strain relaxation at oxide heterointerfaces. The vacancy-mediated valence-retaining intermixing found here would provide a pathway for strain relaxation over typical diffusion lengths without altering the typical ionic nature on either side of the interface. This might be a general feature at oxide heterointerfaces.

IV. CONCLUSION

We have investigated by anomalous SXRD the LAO/STO atomic interface structure for one to five unit cell thin films. All the films investigated show La deficiency and contain

many atomic vacancies. Irrespective of the thickness, all the substrates are doped with La, thereby forming charge neutral $\text{Sr}_{1-1.5x}\text{La}_x\text{O}$ layers. From a film thickness of two unit cells, a polar LAO stacking sequence can be identified. The resulting electrostatic energy buildup is partly compensated by a compositional change at the *B* sites in the substrate's terminating TiO_2 layer.

ACKNOWLEDGMENTS

We wish to thank R. Weigel of the MPI-MF for help during the measurements. This work is supported through VENI, VIDII and VICI grants and by the Foundation for Fundamental Research on Matter (FOM), all part of the Netherlands Organization for Scientific Research (NWO).

*v.vonk@science.ru.nl

- ¹A. Ohtomo and H. Y. Hwang, *Nature (London)* **427**, 423 (2004).
- ²N. Reyren, S. Thiel, A. D. Caviglia, L. F. Kourkoutis, G. Hammerl, C. Richter, C. W. Schneider, T. Kopp, A.-S. Ruetschi, D. Jaccard, M. Gabay, D. A. Muller, J.-M. Triscone, and J. Mannhart, *Science* **317**, 1196 (2007).
- ³A. Brinkman, M. Huijben, M. Van Zalk, J. Huijben, U. Zeitler, J. C. Maan, W. G. Van der Wiel, G. Rijnders, D. H. A. Blank, and H. Hilgenkamp, *Nat. Mater.* **6**, 493 (2007).
- ⁴Ariando, X. Wang, G. Baskaran, Z. Q. Liu, J. Huijben, J. B. Yi, A. Annadi, A. R. Barman, A. Rusydi, S. Dhar, Y. P. Feng, J. Ding, H. Hilgenkamp, and T. Venkatesan, *Nat. Commun.* **2**, 188 (2011).
- ⁵S. Thiel, G. Hammerl, A. Schmehl, C. W. Schneider, and J. Mannhart, *Science* **313**, 1942 (2006).
- ⁶M. Huijben, G. Rijnders, D. H. A. Blank, S. Bals, S. V. Aert, J. Verbeeck, G. V. Tendeloo, A. Brinkman, and H. Hilgenkamp, *Nat. Mater.* **5**, 556 (2006).
- ⁷N. Nakagawa, H. Y. Hwang, and D. A. Muller, *Nat. Mater.* **5**, 204 (2006).
- ⁸W. Siemons, G. Koster, H. Yamamoto, W. A. Harrison, G. Lucovsky, T. H. Geballe, D. H. A. Blank, and M. R. Beasley, *Phys. Rev. Lett.* **98**, 196802 (2007).
- ⁹A. Kalabukhov, R. Gunnarsson, J. Borjesson, E. Olsson, T. Claeson, and D. Winkler, *Phys. Rev. B* **75**, 121404 (2007).
- ¹⁰G. Herranz, M. Basletic, M. Bibes, C. Carretero, E. Taffra, E. Jacquet, K. Bouzouhane, C. Deranlot, A. Hamzic, J.-M. Broto, A. Barthelemy, and A. Fert, *Phys. Rev. Lett.* **98**, 216803 (2007).
- ¹¹P. R. Willmott, S. A. Pauli, R. Herger, C. M. Schlepütz, D. Martoccia, B. D. Patterson, B. Delley, R. Clarke, D. Kumah, C. Cionca, and Y. Yacoby, *Phys. Rev. Lett.* **99**, 155502 (2007).
- ¹²S. A. Chambers, M. H. Engelhard, V. Shutthanandan, Z. Zhu, T. C. Droubay, L. Qiao, P. V. Sushko, T. Feng, H. D. Lee, T. Gustafsson, E. Garfunkel, A. B. Shah, J.-M. Zuo, and Q. M. Ramasse, *Surf. Sci. Rep.* **65**, 317 (2010).
- ¹³R. Pentcheva and W. E. Pickett, *Phys. Rev. Lett.* **102**, 107602 (2009).
- ¹⁴S. A. Pauli, S. J. Leake, B. Delley, M. Bjorck, C. W. Schneider, C. M. Schlepütz, D. Martoccia, S. Paetel, J. Mannhart, and P. R. Willmott, *Phys. Rev. Lett.* **106**, 036101 (2011).
- ¹⁵Z. Zhong, P. X. Xu, and P. J. Kelly, *Phys. Rev. B* **82**, 165127 (2010).
- ¹⁶L. Zhang, X.-F. Zhou, H.-T. Wang, J.-J. Xu, J. Li, E. G. Wang, and S.-H. Wei, *Phys. Rev. B* **82**, 125412 (2010).
- ¹⁷G. Berner, S. Glawion, J. Walde, F. Pfaff, H. Hollmark, L. C. Duda, S. Paetel, C. Richter, J. Mannhart, M. Sing, and R. Claessen, *Phys. Rev. B* **82**, 241405(R) (2010).
- ¹⁸L. Qiao, T. Droubay, T. Kaspar, P. Sushko, and S. Chambers, *Surf. Sci.* **605**, 1381 (2011).
- ¹⁹G. Koster, B. L. Kropman, G. Rijnders, D. H. A. Blank, and H. Rogalla, *Mater. Sci. Eng. B* **56**, 209 (1998).
- ²⁰A. Stierle, A. Steinhäuser, A. Rühm, F. U. Renner, R. Weigel, N. Kasper, and H. Dosch, *Rev. Sci. Instrum.* **75**, 5302 (2004).
- ²¹E. Vlieg, *J. Appl. Crystallogr.* **31**, 198 (1998).
- ²²For the anomalous data, the La atomic scattering factor is corrected by $f' = -10.8$ and $f'' = 14.3$. See Ref. 24 for details about the data analysis.
- ²³E. Vlieg, *J. Appl. Crystallogr.* **33**, 401 (2000).
- ²⁴V. Vonk, *J. Appl. Crystallogr.* **44**, 1217 (2011).
- ²⁵See Supplemental Material at <http://link.aps.org/supplemental/10.1103/PhysRevB.85.045401> for the details of the data reduction, analysis, and atomic positions.
- ²⁶C. Howard and Z. Zhang, *J. Phys. Condens. Matter* **15**, 4543 (2003).
- ²⁷C. Howard, B. Kennedy, and B. Chakoumakos, *J. Phys. Condens. Matter* **12**, 349 (2000).
- ²⁸P. Bouvier and J. Kreisel, *J. Phys. Condens. Matter* **14**, 3981 (2002).
- ²⁹K. Gomann, G. Bocharde, M. Schulz, A. Gomann, W. Maus-Friedrichs, B. Lesage, O. Kaitasov, S. Hoffman-Eifert, and T. Schneller, *PCCP* **7**, 2053 (2005).
- ³⁰U. Balachandran and N. Eror, *J. Electrochem. Soc.* **129**, 1021 (1982).
- ³¹R. Meyer, R. Waser, J. Helmbold, and G. Borchardt, *J. Electrochem. Soc.* **9**, 103 (2002).
- ³²V. Vonk, M. Huijben, K. J. I. Driessen, P. Tinnemans, A. Brinkman, S. Harkema, and H. Graafsma, *Phys. Rev. B* **75**, 235417 (2007).
- ³³For x-ray scattering, these two are indistinguishable as long as the island size is smaller than the x-ray coherence length.
- ³⁴C. H. Lanier, J. M. Rondinelli, B. Deng, R. Kilaas, K. R. Poepelmeier, and L. D. Marks, *Phys. Rev. Lett.* **98**, 086102 (2007).
- ³⁵M. McGibbon, N. Browning, M. Chisholm, A. McGibbon, S. Pennycook, V. Ravikumar, and V. Dravid, *Science* **266**, 102 (1994).
- ³⁶A. S. Kalabukhov, Y. A. Boikov, I. T. Serenkov, V. I. Sakharov, V. N. Popok, R. Gunnarsson, J. Borjesson, N. Ljustina, E. Olsson, D. Winkler, and T. Claeson, *Phys. Rev. Lett.* **103**, 146101 (2009).
- ³⁷D. A. Freedman, D. Roundy, and T. A. Arias, *Phys. Rev. B* **80**, 064108 (2009).